

## Spin Dependent Electrochemistry:

### enantio-selectivity driven by chiral induced spin selectivity effect.

Mirko Gazzotti<sup>1</sup>, Serena Arnaboldi<sup>2</sup>, Sara Grecchi<sup>2</sup>, Roberto Giovanardi<sup>1</sup>, Maria Cannio<sup>1</sup>, Luca Pasquali<sup>1,#,\$</sup>,  
Agnese Giacomino<sup>3</sup>, Ornella Abollino<sup>4</sup>, Claudio Fontanesi<sup>1\*</sup>

<sup>1</sup>*Department of Engineering 'Enzo Ferrari', University of Modena and Reggio Emilia, Via Vivarelli 10,  
41125 Modena, Italy*

<sup>2</sup>*Department of Chemistry, University of Milan, Via Golgi 19, 20133 Milano, Italy*

<sup>3</sup>*Department of Drug Science and Technology, University of Torino, Via Giuria 9, 10125 Torino, Italy*

<sup>4</sup>*Department of Chemistry, University of Torino, Via Giuria 5, 10125 Torino, Italy*

<sup>#</sup>*IOM-CNR, s.s. 14, Km. 163.5 in AREA Science Park, 34149 Basovizza, Trieste, Italy*

<sup>\$</sup>*Department of Physics, University of Johannesburg, P.O. Box 524, Auckland Park 2006, South Africa*

## 1. WORKING ELECTRODES MATERIAL

Ni has been selected because of his ferromagnetic characteristics. Magnetic field modifies the Density of States (DOS) in a ferromagnetic material. This modification, breaks the symmetry of DOS, increases the density of state of one spin orientation near Fermi's level and decrease the other one, so, differently from the unmodified status, it's energetically advantageous for the system to inject electrons with spin polarized population.

In Figure SI an example of the effect of the magnetic field on Ni. Arrows show the spin of the electrons, in red graphs can be seen that there's a variation in density of states (DOS) as described before. In this case, electrons that are going to be injected from the surface will preferably be the ones that have spin UP↑. If we invert the magnetic field, also the modification will be inverted, leading to an higher probability of injection of spin UP↓ electrons.

Spin polarization can be calculated with the simple formula:

$P_n = \frac{n_{\uparrow} - n_{\downarrow}}{n_{\uparrow} + n_{\downarrow}}$	(1)
---	-----

So, if  $P_n = 1$ , electrons are 100% UP, if  $P_n = 0$ , electrons have the same population for both orientation (50% UP - 50% DOWN) and if  $P_n = -1$  the population is 100% electrons with DOWN spin-orientation.

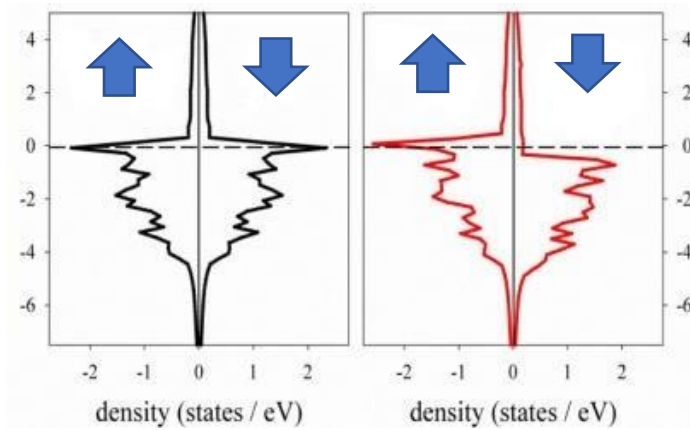


Figure 1SI - Energy vs density of state (DOS) of electrons in the Ni without the magnetic field (black) and with a magnetic field (red). The blue arrow represent the spin of the electrons in the side of the graph

The study of the electron's spin, known as spintronic, is developed due to its use into electronic devices as way to elaborate and, above all, store data due to its nature; spin has only two orientations, so it's assimilable to a binary information, that candidate this property to be used as indicator of the value of a certain bit.

Electrodes in spintronic solid-state devices are made of ferromagnetic material because of the spin must have the same direction. The choice of the ferromagnetic material for electrodes is also to control the information carrier, that are the electrons, in fact that is made by interaction with an external magnetic field. One of the most used effect of the coupling of ferromagnetic film is the Giant Magnetoresistance (GMR), an effect of thin ferromagnetic films alternate with non-ferromagnetic metal film, as in Figure 2SI, where the orientation of magnetic fields in the external layers cause a change in the resistance of the spin-valve; if the magnetic field are aligned the resistance drops, current pass and so the signal; if are antiparallel it increases and the current cannot pass. The information is deduced through the current, so if the polarization is parallel the cell has a value of "1", if it's not it's a "0".

Normally one of the film has a permanent magnetization and, in the other one, the verse of the magnetization can be switched with a small external magnetic field.

Those elements are used as memory devices, where informations are stored not with electric charge but with magnetic field.

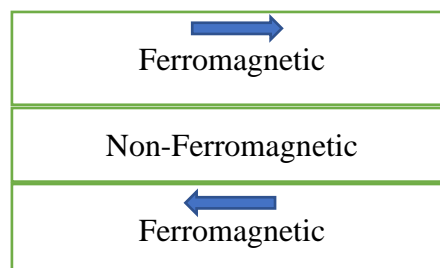


Figure 2SI - Scheme of construction of a Spinfilter device (spin-valve) under and antiparallel magnetic field (represented by the blue arrow). This situation is coded as a "0"

This situation is researched because the Ni and the chiral molecules could work as a sort of polarizing filters, in fact if the side of the magnet work as increaser of population of one spin-orientation and the chiral molecule stops that orientation, the current measured during the experiment should be lower than the one read from the one measured on the other pole of the magnet in the same operative condition.

Glassy Carbon (GC) plates (2.5 cm × 2.5 cm × 1 mm) purchased from HTW (SIGRADUR G) and Platinum (Pt) wire 0.5 mm in diameter, Sigma Aldrich. For the CV of Fe(II)/Fe(III) was used as working electrode surfaces made of evaporated ( $10^{-6}$  torr) gold (Au) or nickel(Ni) (300 nm) layer on top of 5 nm Ti adhesion layer, grown on a single crystal silicon, Si (100) ( $400 \Omega/\text{cm}^2$ ) of  $525 \pm 25 \mu\text{m}$  thickness (300 nm of thermal oxide on the surface), the latter was purchased from University Wafers, Inc. All metals (Ni, Au, Ti) used during evaporation were purchased from Kurt J. Lesker.

The copper (Cu) is Cu – DHP (Deoxidized High residual Phosphorus) a commercial pure copper for pipes that is free of oxygen and has relative high percentage of phosphorus (P between 0.015% and 0.04%). It has been purchased from Commerciale Fond s.p.a.

The solution of Fe(II)/Fe(III) was made from  $\text{K}_4\text{Fe}(\text{CN})_6$  and  $\text{K}_3\text{Fe}(\text{CN})_6$ , both purchased from Sigma Aldrich.

## 2. Ni ELECTRODEPOSITION FROM WATT'S BATH

Ni electrodeposition has been carried out in a WB solution, under potentiostatic regime, at -1.4 V constant potential for 900 seconds. Figure 3SI and Figure 4SI set out a typical current vs time curve obtained during the electrodeposition.

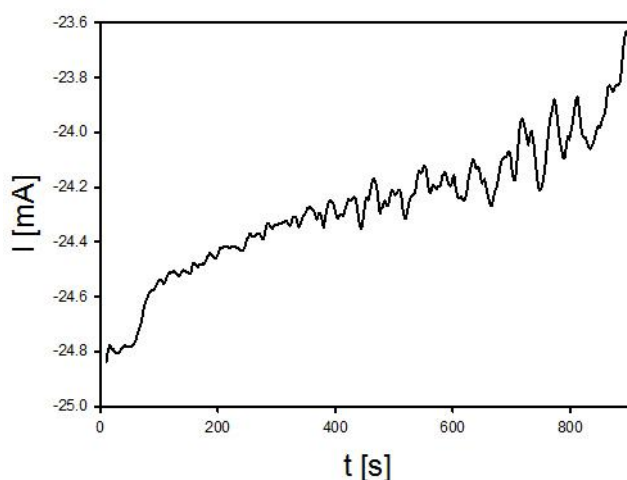


Figure 3SI. Ni electrodeposition, chronoamperometry, Watt's bath -1.4 V.

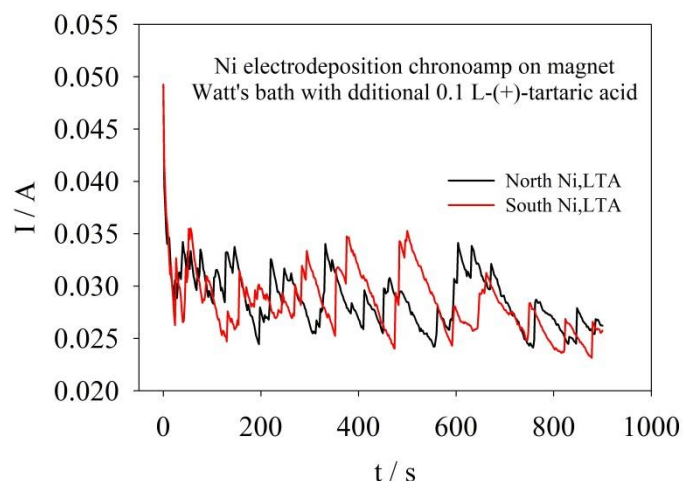


Figure 4SI. Ni electrodeposition, chronoamperometry, Watt's bath with 0.1 M L-(+)-tartaric acid addition, - 1.4 V. Black curve: north side of the magnet. Red curve: south side of the magnet

## 2.1 ON COPPER

Surface's quality of Ni obtained via electrodeposition under potentiostatic or galvanostatic regime where compared, potentiostatic conditions were selected because of the results were more constant.

Figure 1SI shows the layer of the Ni electrodeposited on Cu in galvanostatic regime at -20 mA for 2700 s on a substrate of Cu. The thickness of the layer is approximately 100  $\mu\text{m}$ . On the left bottom of the Figure 1SI there's the edge of the deposit, that appears almost perpendicular to the surface of Cu so it's easy to measure the thickness.

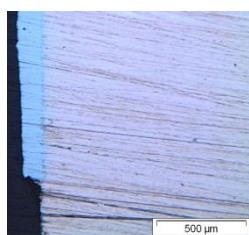
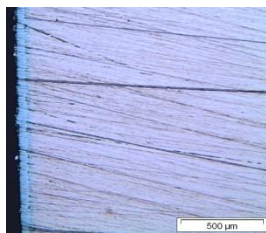


Figure 1SI - Photo at 50x of Ni electrodeposited (blue) on Cu in galvanostatic regime at - 20 mA for 2700 s

Figure 2SI shows the layer of the Ni electrodeposited on Cu in galvanostatic regime (blue on the left) at -10 mA for 2700 s on a substrate of Cu. The thickness of the layer is approximately 50  $\mu\text{m}$ . This is coherent with the Figure 1SI where the current is the double, so the charge exchanged leads to a double quantity of atoms reduced on the surface.

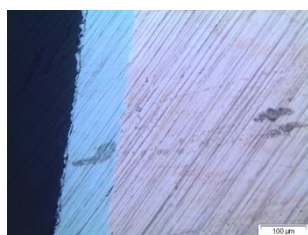


*Figure 2SI - Photo at 50x of Ni electrodeposited (grey) on Cu in galvanostatic regime at -10 mA for 2700 s*

The galvanostatic regime didn't give constant result for what concerns the current during the electrodeposition, so, the regime of deposition has been change to potenziostatic and has been that for all the depositions in this thesis.

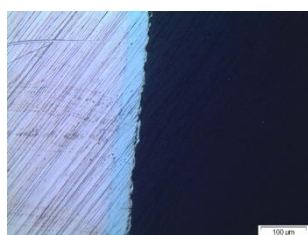
Depositions were made at -1300 mV, -1500 mV and -1900 mV on the Cu to measure thickness and evaluate the aspect of Ni deposited.

Figure 3SI shows the layer of Ni deposited on Cu at -1300 mV (blue on the left), deposition lasted 2700 seconds. The thickness is approximately 100 μm. It's possible to see that the Ni has a good adhesion to the Cu and the layer is continuous and has a constant thickness.



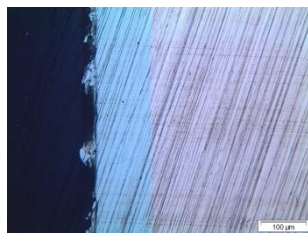
*Figure 3SI - Photo at 200x of Ni electrodeposited (blue) on Cu potenziostatic regime at -1300 mV for 2700 s*

Figure 4SI shows the layer of Ni deposited on Cu at -1500 mV (blue on the centre), the deposition lasted 2700 seconds. The thickness is approximately 100 μm.



*Figure 4SI - Photo at 200x of Ni electrodeposited (blue) on Cu potenziostatic regime at -1500 mV for 2700 s*

Figure 5SI shows the thickness of Ni deposited on Cu at -1900 mV (blue on the centre), the deposition lasted 2700 seconds. The thickness is approximately 120 μm and this is coherent with the higher current during deposition's process.



*Figure 5SI - Photo at 200x of Ni electrodeposited (blue) on Cu potenziostatic regime at -1900 mV for 2700 s*

After those experiment for the determination of the right voltage to make a good deposition, it has been searched the lower amount of time to achieve a continuous layer of Ni enough thick for the successive experiment of water splitting. For the previous experiments (Figure 1SI to Figure 5SI), the duration of the deposition was always 2700 s, equals to 45 minutes. After those, were tested shorter durations: 1800 s and 900 s, equal respectively to 30 and 15 minutes. Quality of deposition was valuated with the comparison with the CV of Ni evaporated (Figure 23SI); more defined were the characteristic peaks of Ni, better was the deposition.

## **1.2 On gold**

After the previous experiments on Cu to determine the better operative conditions, that from now on will be: electrodeposition in potentiostatic regime at -1400 mV for 900 s, we changed the substrate to Au to measure the efficiency of deposition. Has been calculated the percentage of current that reduced the Ni in the WB into metallic Ni on the substrate surface. To do so, we used the Figure S graph, that describes the current necessary to maintain the imposed potential during the time required for the deposition. The area underlying the curve is the charge exchanged.

After the measurement of the weight of the deposit and the charge exchanged is possible to determine the efficiency of the deposition and, with a simple operation, also the presence and the percentage of any parasite reactions. In fact, every exchanged charge that isn't involved in the reduction of Ni is considerable part of parasite reaction that effect negatively the deposition.

The deposit on Au weight:  $0.0062 \pm 0.0001$  g.

The charge exchanged is provided from GPES software that control the deposition process and is equal to: 21.8 C.

Considering the charge of the electron  $e^- = -1.602 \cdot 10^{-19}$  the number of exchanged electrons are:

$$\frac{21.8 \text{ C}}{1.602 \cdot 10^{-19} \text{ C}} = 1.3608 \cdot 10^{20}$$

That divide for 2 because every atom of Ni required 2  $e^-$  for the reduction reactions leads to:  $6.804 \cdot 10^{19}$  atoms of Ni. This number, divided for the  $N_a$ , Avogadro's number ( $6.022 \cdot 10^{23}$ ), is the number of moles of Ni reduced:

$$\frac{6.804 \cdot 10^{19} \text{ atoms}}{6.022 \cdot 10^{23} \frac{\text{atoms}}{\text{mol}}} = 1.1299 \cdot 10^{-4} \text{ mol}$$

This value, multiplied for the atomic weight of the Ni (58.91 g/mol) gives the maximum mass of Ni reduced in the experiment:

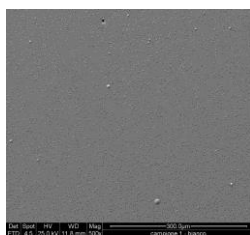
$$1.1299 \cdot 10^{-4} \text{ mol} \cdot 58.91 \frac{\text{g}}{\text{mol}} = 6.65598 \cdot 10^{-3} \text{ g}$$

So, the efficiency of the deposition is:

$$\frac{6.2 \cdot 10^{-3} g}{6.65598 \cdot 10^{-3} g} = 0.9315 = 93.15 \%$$

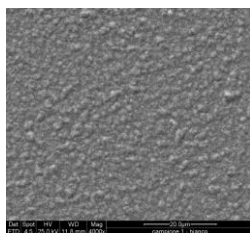
During the deposition, is noticeable the production of gas from the surface of the deposit, this gas is  $H_2$  and from the efficiency of the reduction of Ni, if this is the only parasite reaction, can be found the quantity of  $H_2$  produced.

Figure 6SI shows the surface images as obtained using ESEM microscopy, of Ni electrodeposited on evaporated Au on a wafer of Si done for the efficiency measurement.



*Figure 6SI - Photo taken at ESEM microscope at 500x of the surface of Ni electrodeposited at -1400 mV for 900 s on Au evaporated on a wafer of Si*

Figure 7SI shows the same surface as Figure 6SI but at a higher magnification. The surface is characterized from the presence of a pattern of hemisphere equally distributed.



*Figure 7SI - Photo taken at ESEM microscope at 4000x of the surface of Ni electrodeposited at -1400 mV for 900 s on Au evaporated on a wafer of Si*

In Figure 25SI is calculated the effective area of the Ni electrodeposited used in this chapter in relation to a Ni evaporated surface.

### 2.3 Ni deposited on magnet

In Figure 8SI there's a graph and the geometrical specifications of the magnet. The measurements are in inches, so for the SI the measures are 2.54 cm (thickness) x 1.27 cm (width) x 1.27 cm (length).

It's a neodymium (Nd) magnet, N42 is an international grade for magnet that represents the strength of magnets, the maximum grade is N52. The magnet is nickel coated.

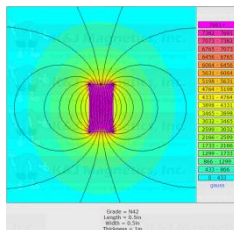


*Figure 8SI - Scheme of the magnetic field and geometrical spec in the magnet B88X0 of K&J Magnets, Inc*

Figure 9SI shows the surface of Ni electrodeposited directly on the magnet. This surface hasn't been in contact with different solution neither has made CVs with them, it's just deposited and then removed from the magnet to be watched at the ESEM microscope (Figure 11SI sample 4).

In comparison to Figure 7SI, there isn't the characteristic presence of the hemisphere on the surface, but retrace the substrate, so the surface appears flatter in areas where the substrate is free of scratch or irregularity.

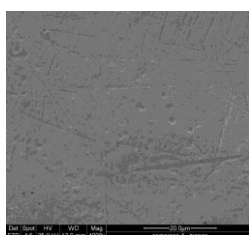
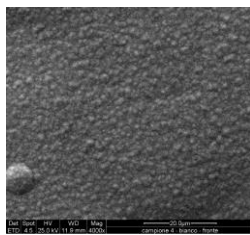


*Figure 9SI - Photo taken at ESEM microscope at 4000x of the surface, in contact with the surface of the magnet, of Ni electrodeposited at -1400 mV for 900 s on the north surface of the magnet*

Figure 10SI shows the opposite surface of Figure 9SI, which is the one exposed to the environment. Also, this one hasn't been in contact with any other solution than the WB, so this is the white samples used to confront effects of repeated CVs in different solutions.

The surface is like the one found in Figure 7SI, strongly suggesting that quality of the electrodeposited Ni is independent of the magnetic field.



than in the other comparison, so, join to the similarity of ESEM images, lead us to say that the L-(+)-Tartaric Acid has a role in the increasing of the peaks' current and that increasing isn't due to the increase of WE's area.

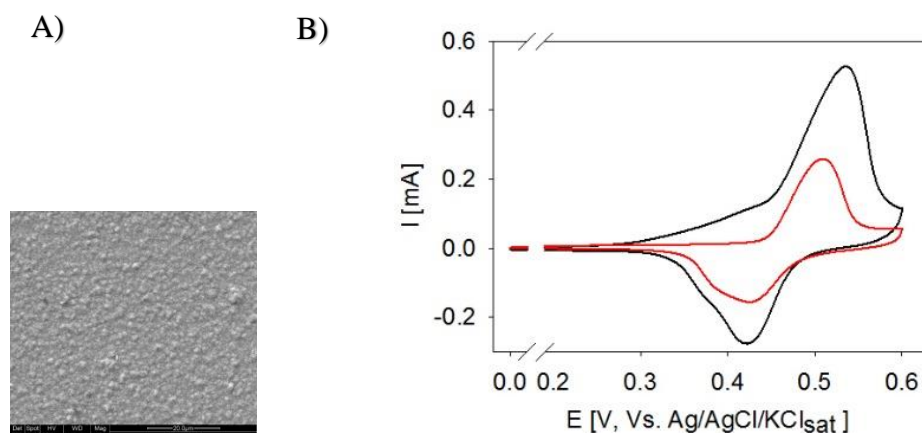


Figure 12SI – A) Photo taken at ESEM microscope at 4000x of the surface of the Ni deposited on Au after the CVs with KOH 0.1 M before (red on the B) graph) and L-(+)-Tartaric Acid 0.5 mM in KOH 0.1 M after (black on the B) graph)

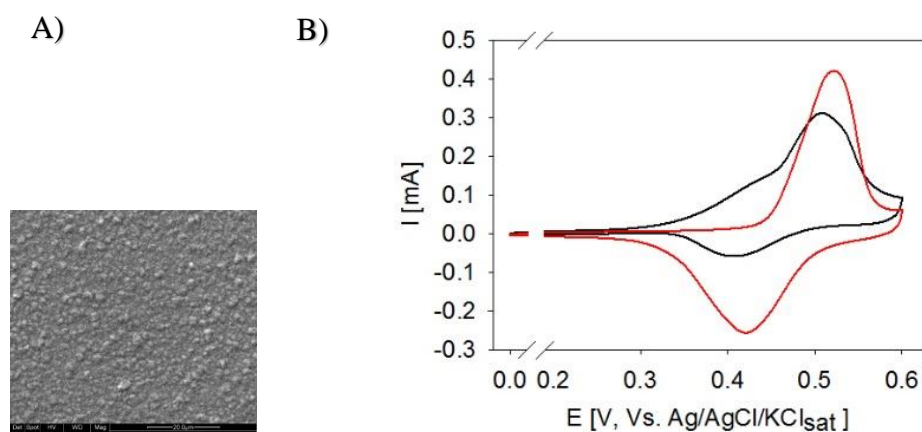
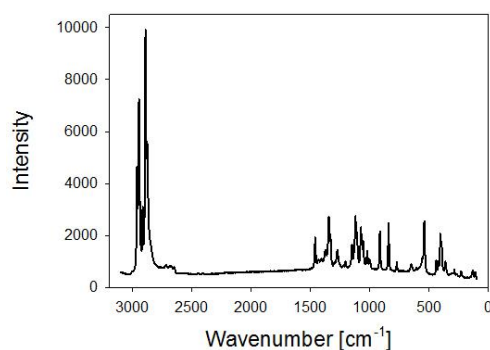


Figure 13SI – A) Photo taken at ESEM microscope at 4000x of the surface of the Ni deposited on Au after the CVs with L-(+)-Tartaric Acid 0.5 mM in KOH 0.1 M before (black on the B) graph) and KOH 0.1 M after (red on the B) graph)

## Raman results

We tested the surface of some Ni electrodeposited on the magnet that worked with the solution of L-(+)-Tartaric Acid and D-(+)- Glucose to reveal if there's organic compound adsorbed from the surface.

First thing to do in a Raman analysis is the acquisition of the Raman spectra of the searched substances; in Figure 14SI and Figure 15SI the spectrum of D-(+)- Glucose and L-(+)-Tartaric Acid respectively.



*Figure 14SI - Raman spectrum of D-(+)- Glucose taken with green laser with a wavelength of 532.05 nm and 50 mW of power*

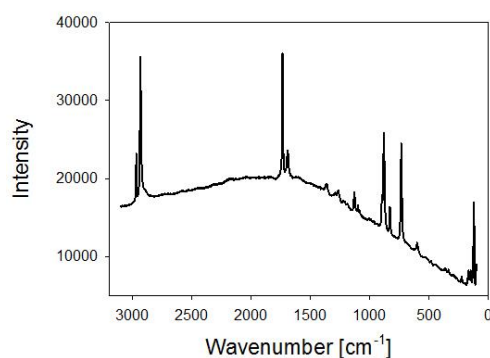


*Figure 15SI - Raman spectrum of L-(+)-Tartaric Acid taken with green laser with a wavelength of 532.05 nm and 50 mW of power*

The following figures report the Raman spectra of the Ni deposited on the poles of the magnet after the CVs with the solutions of L-(+)-Tartaric Acid 0.5 mM in KOH 0.1 M and D-(+)- Glucose 0.1 M in KOH 0.1 M. Figure 16SI shows the Raman spectrum of the surface of Ni electrodeposited on the north pole of the magnet after being detached from it and after the CVs with the L-(+)-Tartaric Acid solution with potential between 0 and 0.8 V.

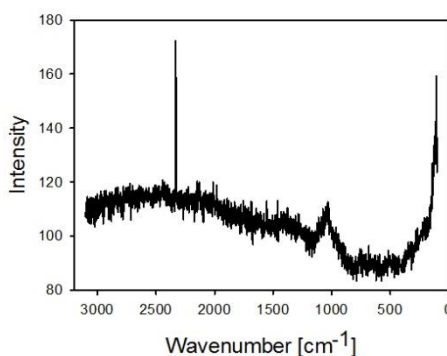


*Figure 16S - Raman spectrum of the Ni electrodeposited on the north pole of the magnet B88X0 of K&J Magnet, Inc after the CVs with the solution of L-(+)-Tartaric Acid 0.5 mM in KOH 0.1 M. The spectrum was taken with green laser at 532.04 nm with 50 mW of power*

Figure 17SI shows the Raman spectrum of the surface of Ni electrodeposited on the south pole of the magnet after being detached from it and after the CVs with L-(+)-Tartaric Acid solution with potential between 0 and 0.8 V.

In comparison with Figure 15SI, neither the north or the south deposit has adsorbed the L-(+)-Tartaric Acid because there aren't the characteristic peaks of L-(+)-Tartaric Acid in the spectra (Figure 16SI and Figure 17SI).

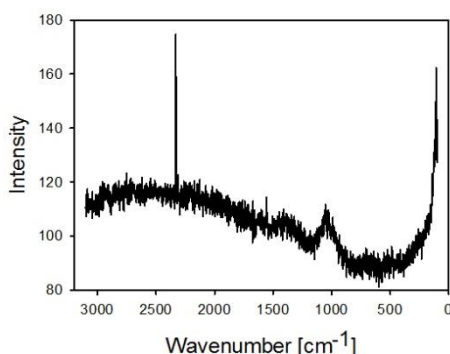


*Figure 17SI - Raman spectrum of the Ni electrodeposited on the south pole of the magnet B88X0 of K&J Magnet, Inc after the CVs with the solution of L-(+)-Tartaric Acid 0.5 mM in KOH 0.1 M. The spectrum was taken with green laser at 532.04 nm with 50 mW of power*

Figure 18S shows Raman spectrum of the surface of Ni electrodeposited on the north pole of the magnet after being detached from it and after the CVs with the D-(+)- Glucose solution with potential between 0 and 0.8 V.

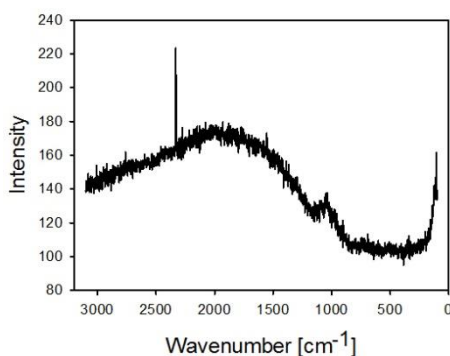


*Figure 18SI - Raman spectrum of the Ni electrodeposited on the north pole of the magnet B88X0 of K&J Magnet, Inc after the CVs with the solution of D-(+)- Glucose 0.1 M in KOH 0.1 M. The spectrum was taken with green laser at 532.04 nm with 50 mW of power*

Figure 19SI shows the Raman spectrum of the surface of Ni electrodeposited on the south pole of the magnet after being detached from it and after CVs with the D-(+)- Glucose solution with potential between 0 and 0.8 V.

In comparison with Figure 14SI, neither the north or the south deposit has adsorbed the D-(+)- Glucose because there aren't the characteristic peaks of the D-(+)- Glucose in the spectra (Figure 18SI and Figure 19SI).

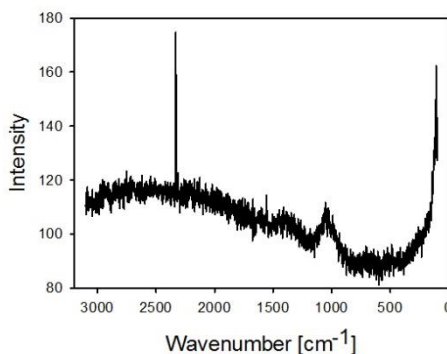


Figure 19SI - Raman spectrum of the Ni electrodeposited on the south pole of the magnet B88X0 of K&J Magnet, Inc after the CVs with the solution of D-(+)- Glucose 0.1 M in KOH 0.1 M. The spectrum was taken with green laser at 532.04 nm with 50 mW of power

### Fe(II)/Fe(III) cyclic voltammetry

To assess the quality of the surface of Ni electrodeposited have been made CVs in Fe(II)/Fe(III) 5 mM in KCl 0.1M.

CVs were measured on Ni deposited on Au evaporated on a Si (100) wafer (used as WE), and the test was repeated before and after a set of CVs in KOH 0.1 M solution between 0 and 0.8 V, to measure the eventual increase of area of the WE considering that the area of the electrode is directly proportional to the current.

Figure 20SI shows two different CVs associated to Ni deposited on Au. For both curves the peaks are at 140 mV in reduction and 350 mV in oxidation so the gap between peaks is 210 mV, that in comparison to the Figure 27SI, leads to think that the surface has a good quality.

The highness of peaks is slightly different in the backward scan where the red one has a current of -0.5 mA against the -0.46 mA of the black one. This means that there're more oxidation reactions after the treatment with KOH than in the surface untreated, so the area is higher.

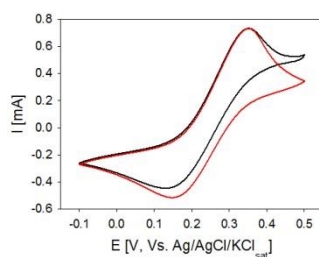


Figure 20SI - Comparison between the CV of Ni electrodeposited on Au in a solution of Fe(II)/Fe(III) 5 mM in KCl 0.1 M before (black) and after (red) the CVs in a solution of KOH 0.1 M between 0 and 0.8 V. All the tests were made at 50 mV/s with Pt as CE

Figure 21SI shows the same experiment of the Figure 20SI but on a different WE, in this case the WE is Ni electrodeposited on south pole of a magnet. Differently from Figure 20SI, the difference before and after the treating is greater, especially in the backward scan where the black one, that is the curve related to the measurement done before the CVs with KOH, hasn't the peak relative to the oxidation reaction.

Judging by the shape of the curves from Figure 20SI and Figure 21SI and from the values of the areas in the Table SI, seems that the CVs with the KOH adjust the surface of Ni making them more homogeneous and with a better quality, in fact the ratio between areas are closer to 1, that leads to think that the surface undergoes oxidation process, in fact the ratio between charge exchanged in oxidation is on the 75% of the time higher than the one exchanged in the reduction process, as seen in the Figure 12SI and Figure 13SI.

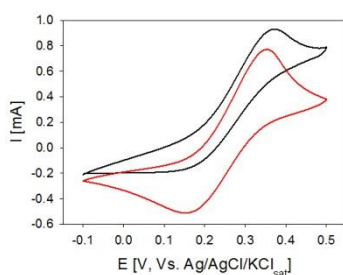
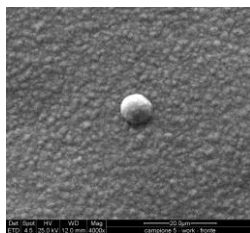


Figure 21SI - Comparison between the CV of Ni electrodeposited on the south pole of a magnet B88X0 of K&J Magnet, inc. in a solution of Fe(II)/Fe(III) 5 mM in KCl 0.1 M before (black) and after (red) the CVs in a solution of KOH 0.1 M between 0 and 0.8 V. All the tests were made at 50 mV/s with Pt as CE

Table ISI shows that the area underlying the scan are close one to another in all the cases, in fact the ratio is always close to one.

Table ISI - Area of the CVs in Figure 20SI and Figure 21SI			
Experiment	Scan	Area [C]	Ratio ( $A_{\text{forward}} / A_{\text{backward}}$ )
Black Graph in Figure 20SI	Forward	0.00398	0.978
	Backward	0.00407	
Red Graph in Figure 20SI	Forward	0.00375	1.014
	Backward	0.00370	
Black Graph in Figure 21SI	Forward	0.00406	1.053
	Backward	0.00386	
Red Graph in Figure 21SI	Forward	0.00377	1.011
	Backward	0.00373	

Figure 22SI shows a SEM image of the Ni electrode surface after recording CVs in the 0 ÷ 0.8 V potential: that is after recording of the CVs shown in Figure 5 of the article. Figure 22SI image must be compared with Figure 10SI to pinpoint any large-scale change induced by the use in the electrochemical measurements. Remarkably, no significant change is present. A further indication that any variation in the CV current is in fact due to variations induced in the OER mechanism by the chiral compounds present in the bulk solution.



*Figure 22SI - Photo taken at ESEM microscope at 4000x of the surface, in contact with the atmosphere, of Ni electrodeposited at -1400 mV for 900 s on the north surface of the magnet*

### Control surfaces: evaporated Ni and Au

In this chapter, there are curves measured in laboratory of surfaces obtained with different and more sophisticated method of deposition, that have been used as comparison with the other curves measured on surfaces electrodeposited. The differences are indicator of the quality of the surfaces.

Figure 23SI shows the CV of Ni evaporated on a wafer of Si (100) in a solution of KOH 0.1 M.

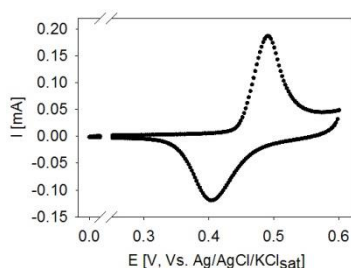


Figure 23SI - CV of Ni evaporated on a wafer of Si as WE in a KOH 0.1 M solution. The test was made at 50 mV/s with Pt as CE

Figure 28SI shows the CV of Ni electrodeposited on a surface of Au evaporated on Si (100)

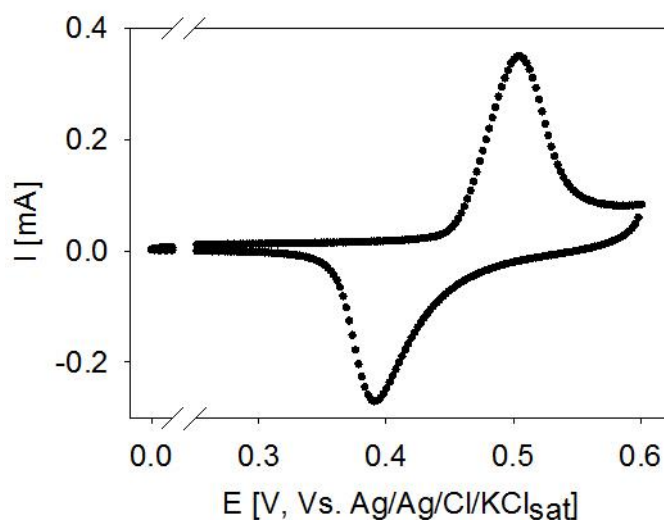


Figure 24SI - CV of Ni electrodeposited on Au on a wafer of Si as WE in a KOH 0.1 M solution. The test was made at 50 mV/s with Pt as CE

Figure 25SI shows the comparison between the previous two CVs (Figure 23SI and Figure 24SI). The difference of current is explicable with the lower area of the evaporated surface, which has a flatter surface due to the method of deposition.

Those measurements can be used to evaluate the effective area of the Ni deposited respect the Ni evaporated. In fact, the area of the forward scan of the CV of the Ni evaporated is equal to  $6.006 \cdot 10^{-4}$  C while for the one evaporated is  $2.876 \cdot 10^{-4}$  C, this means that the charge exchanged during the oxidation process is  $\frac{6.006 \cdot 10^{-4}}{2.876 \cdot 10^{-4}} = 2.088$  times higher in the deposited surface, so the surface is 2.088 times the one evaporated.

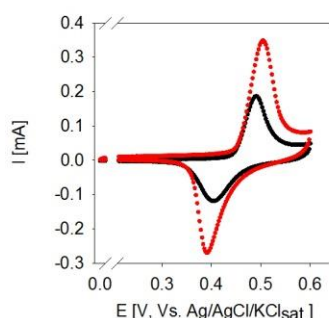


Figure 25SI - Comparison between CV of Ni electrodeposited on Au on Si(100) (Red) and Ni evaporated on Si(100) (Black), used as WE. Both CVs were made at 50 mV/s with Pt as CE

Figure 26SI shows the comparison between a CV of a solution 5 mM of Fe(II)/Fe(III) in KCl 0.1 M with GC as WE and Pt as CE, in black, and a CV fitted by the software based on the data of the experiment, in red.

The redox process associated with the transition between the two oxidation state of Fe (Fe(II)/Fe(III)) that occur during the CV is perfectly reversible, so the curve has two peaks with the same area that theoretically have a gap of potential between maximum and minimum of 58 mV. Here the difference in the black one is of 170 mV, and in the red one is 120 mV. The difference of gap between the theoretical and the measured in an experiment give an idea of the quality of the surface about the conductive property of the surface of the WE, and the current of the peaks a measure of the real area of the WE.

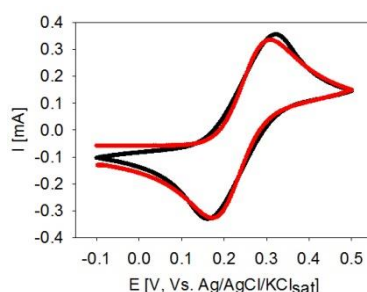
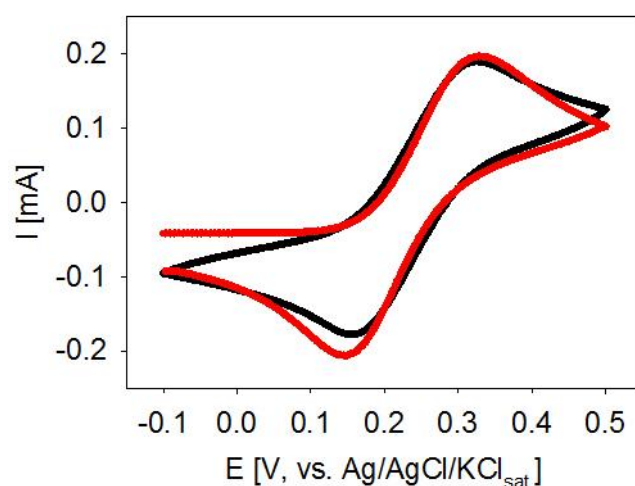


Figure 26SI - Comparison between CV of a solution 5 mM of Fe(II)/Fe(III) in KCl 0.1 M (Black) on a GC surface, used as WE, and a theoretical CV fitted by the software based on the data of the measurement (Red). The scan was made at 50 mV/s with Pt as CE

Figure 27SI shows the comparison between a CV of a solution 5 mM of Fe(II)/Fe(III) in KCl 0.1 M with Au on Si (100) as WE and Pt as CE in black, and a CV fitted by the software based on the data of the experiment, in red. Unlike Figure 26SI the difference between the peaks is lower for the black one (140 mV), and higher for the fitted one (150 mV); also, the current of the peaks are lower so the shapes of the curves are less steep.



*Figure 27SI - Comparison between CV of a solution 5 mM of Fe(II)/Fe(III) in KCl 0.1 M (Black) on Au on Si (100) surface, used as WE, and a theoretical CV fitted by the software based on the data of the measurement (Red). The scan was made at 50 mV/s with Pt as CE*

#### 4. Glucose oxidation

Figure 32SI is an exact reply of Figure 5cd of the main manuscript, which is here reported with a larger magnification, full forward and backward curves and a grid helping in the estimation of the potential and current values from the graph.

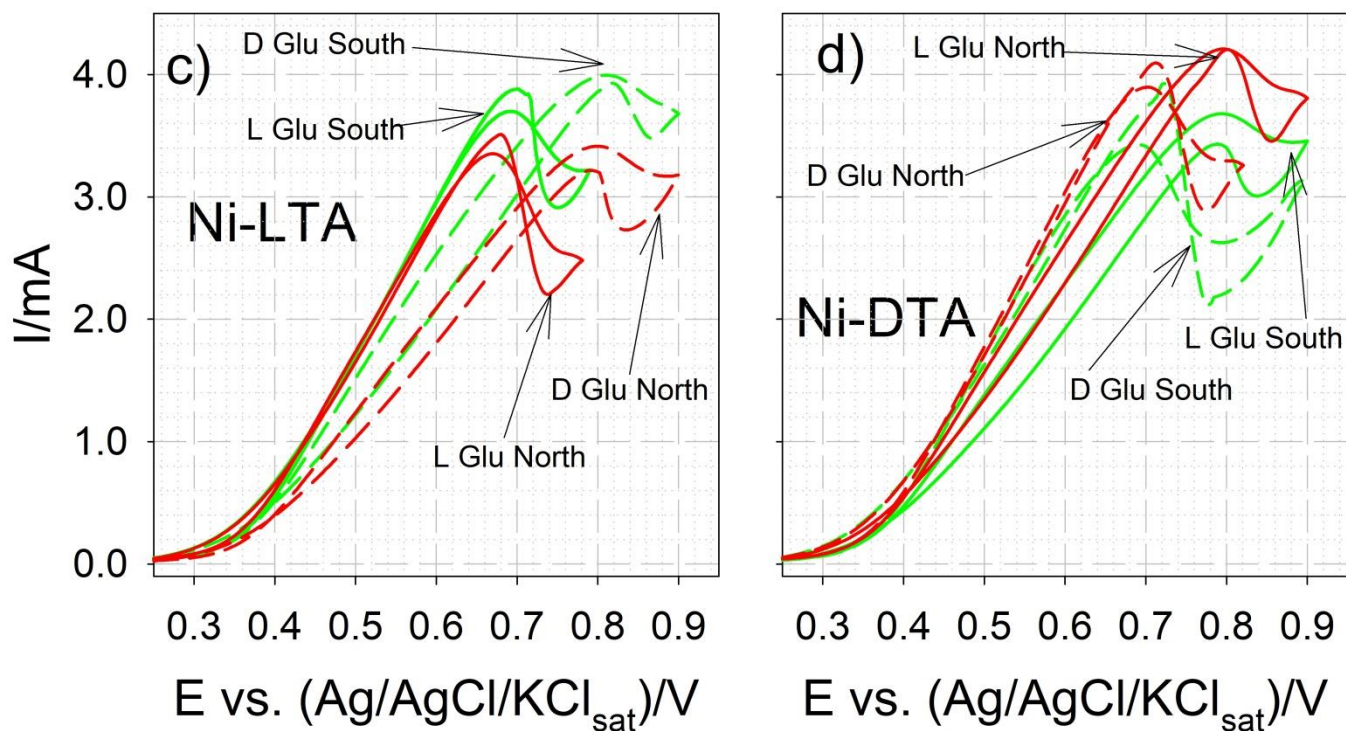


Figure 32SI - CV curves in 0.1 M KOH aqueous solution: c) Ni-LTA WE, north and south, in enantiopure solution of 0.1 M L-glu or D-glu. d) Ni-LDA WE, north and south, in enantiopure solution of 0.1 M L-glu or D-glu. Solid red line: L-glu on north. Dashed red line: D-(+)-glucose on north. Solid green line: L-glu on south. Dashed green line: D-(+)-glucose on south.

Table IISI - Anodic peak current, J, and relevant potential, E, measured for CV on Ni electrodeposited on the magnet. L-(+)-tartaric acid 0.5 mM in KOH 0.1 mM aqueous solution. 50 mV/s scan rate, Ag/AgCl/KCl<sub>sat</sub> as RE and Pt as CE.

	NORTH POLE			
	L-(+)-tartaric acid 0.5 mM in KOH 0.1 M		KOH 0.1 M	
Test Name	J Anodic [A]	E Anodic [V]	J Anodic [A]	E Anodic [V]
CV01_Scan1	6.96E-04	0.569	4.99E-04	0.522
CV01_Scan3	6.18E-04	0.554	3.77E-04	0.510
CV01_Scan5	6.06E-04	0.552	3.90E-04	0.513
CV02_Scan1	6.82E-04	0.559	5.19E-04	0.532
CV02_Scan3	6.38E-04	0.552	4.86E-04	0.522
CV02_Scan5	6.41E-04	0.549	5.08E-04	0.522
CV03_Scan1	7.25E-04	0.554	5.88E-04	0.535
CV03_Scan3	6.74E-04	0.547	5.77E-04	0.527
CV03_Scan5	6.78E-04	0.544	5.94E-04	0.527
	SOUTH POLE			
	L-(+)-tartaric acid 0.5 mM in KOH 0.1 M		KOH 0.1 M	
Test Name	J Anodic [A]	E Anodic [V]	J Anodic [A]	E Anodic [V]
CV01_Scan1	1.20E-03	0.574	9.91E-04	0.544
CV01_Scan3	1.02E-03	0.552	8.65E-04	0.552
CV01_Scan5	1.00E-03	0.549	8.80E-04	0.522
CV02_Scan1	1.13E-03	0.559	9.52E-04	0.530
CV02_Scan3	1.05E-03	0.549	9.21E-04	0.525
CV02_Scan5	1.06E-03	0.547	9.44E-04	0.525
CV03_Scan1	1.28E-03	0.556	1.03E-03	0.532
CV03_Scan3	1.13E-03	0.547	9.95E-04	0.527
CV03_Scan5	1.14E-03	0.547	1.01E-03	0.527

Table III SI- Anodic peak current, J, and relevant potential, E, measured for CV on Ni electrodeposited on the magnet. L-(+)-tartaric acid 0.5 mM in KOH 0.1 mM aqueous solution. 50 mV/s scan rate, Ag/AgCl/KCl<sub>sat</sub> as RE and Pt as CE.

	NORTH POLE			
	L-(+)-tartaric acid 0.5 mM in KOH 0.1 M		KOH 0.1 M	
Test Name	J Anodic [A]	E Anodic [V]	J Anodic [A]	E Anodic [V]
CV01_Scan1	6.49E-04	0.554	3.61E-04	0.525
CV01_Scan3	5.66E-04	0.544	3.14E-04	0.513
CV01_Scan5	5.49E-04	0.542	3.34E-04	0.513
CV02_Scan1	6.26E-04	0.549	3.73E-04	0.518
CV02_Scan3	5.74E-04	0.542	3.76E-04	0.515
CV02_Scan5	5.82E-04	0.542	3.92E-04	0.515
CV03_Scan1	6.48E-04	0.547	4.53E-04	0.518
CV03_Scan3	6.05E-04	0.542	4.63E-04	0.518
CV03_Scan5	6.04E-04	0.540	4.74E-04	0.518
	SOUTH POLE			
	L-(+)-tartaric acid 0.5 mM in KOH 0.1 M		KOH 0.1 M	
Test Name	J Anodic [A]	E Anodic [V]	J Anodic [A]	E Anodic [V]
CV01_Scan1	7.27E-04	0.570	4.80E-04	0.601
CV01_Scan3	6.48E-04	0.559	4.06E-04	0.537
CV01_Scan5	6.36E-04	0.557	4.26E-04	0.535
CV02_Scan1	7.11E-04	0.566	5.01E-04	0.547
CV02_Scan3	6.58E-04	0.562	4.67E-04	0.537
CV02_Scan5	6.51E-04	0.559	4.79E-04	0.537
CV03_Scan1	6.92E-04	0.564	5.22E-04	0.549
CV03_Scan3	6.60E-04	0.559	5.14E-04	0.542
CV03_Scan5	6.70E-04	0.559	5.26E-04	0.540

Table IVSI - Ratio of anodic current peaks, measured for CV on Ni electrodeposited on the magnet. 0.5 mM L-(+)-tartaric acid in KOH 0.1 M aqueous solution. 50 mV/s scan rate. Last column shows the result of the sign function of the difference between the two values in the associated row (North – South)

	ANODIC CURRENT RATIO		sgn ( J <sub>ratio</sub> North - J <sub>ratio</sub> South)
	J <sub>ratio</sub> North	J <sub>ratio</sub> South	
Test Name	J <sub>Tart</sub> / J <sub>KOH</sub>	J <sub>Tart</sub> / J <sub>KOH</sub>	
CV01_Scan1	1.798	1.514	+
CV01_Scan3	1.799	1.596	+
CV01_Scan5	1.646	1.492	+
CV02_Scan1	1.677	1.420	+
CV02_Scan3	1.529	1.410	+
CV02_Scan5	1.487	1.359	+
CV03_Scan1	1.432	1.326	+
CV03_Scan3	1.305	1.285	+
CV03_Scan5	1.276	1.273	+
CV01_Scan1	1.798	1.514	+
CV01_Scan3	1.799	1.596	+
CV01_Scan5	1.646	1.492	+
CV02_Scan1	1.677	1.420	+
CV02_Scan3	1.529	1.410	+
CV02_Scan5	1.487	1.359	+
CV03_Scan1	1.432	1.326	+
CV03_Scan3	1.305	1.285	+
CV03_Scan5	1.276	1.273	+

Table VSI - Values of peaks of anodic current during the CV on Ni electrodeposited on both side of the magnet B88X0 of K&J Magnet, Inc that acts as WE followed the potentials at which occurs, for both the electrolytes support that has been tested, D-(-)-tartaric acid 0.5 mM in KOH 0.1 mM aqueous solution and KOH 0.1 M aqueous solution. All the CVs are made with Ag/AgCl/KCl<sub>sat</sub> as RE and Pt as CE, with a scan rate of 50 mV/s

	NORTH POLE			
	D-(-)-tartaric acid 0.5 mM in KOH 0.1 M		KOH 0.1 M	
	J Anodic [A]	E Anodic [V]	J Anodic [A]	E Anodic [V]
CV01_Scan1	3.85E-04	0.600	2.61E-04	0.600
CV01_Scan3	3.60E-04	0.600	2.31E-04	0.600
CV01_Scan5	3.52E-04	0.600	2.30E-04	0.600
CV02_Scan1	8.20E-04	0.700	5.44E-04	0.684
CV02_Scan3	7.53E-04	0.688	5.27E-04	0.659
CV02_Scan5	7.45E-04	0.686	5.49E-04	0.659
CV03_Scan1	7.76E-04	0.688	5.88E-04	0.664
CV03_Scan3	7.29E-04	0.686	5.48E-04	0.659
CV03_Scan5	7.27E-04	0.688	5.52E-04	0.662
	SOUTH POLE			
	D-(-)-tartaric acid 0.5 mM in KOH 0.1 M		KOH 0.1 M	
	J Anodic [A]	E Anodic [V]	J Anodic [A]	E Anodic [V]
CV01_Scan1	3.85E-04	0.600	2.75E-04	0.600
CV01_Scan3	2.96E-04	0.600	1.77E-04	0.600
CV01_Scan5	2.78E-04	0.600	1.66E-04	0.600
CV02_Scan1	5.73E-04	0.679	3.30E-04	0.675
CV02_Scan3	5.23E-04	0.667	3.10E-04	0.649
CV02_Scan5	5.19E-04	0.664	3.26E-04	0.647
CV03_Scan1	6.14E-04	0.676	3.91E-04	0.657
CV03_Scan3	5.52E-04	0.671	3.60E-04	0.649
CV03_Scan5	5.53E-04	0.671	3.71E-04	0.652

Table IISI - Values of peaks of anodic current during the CV on Ni electrodeposited on both side of the magnet B88X0 of K&J Magnet, Inc that acts as WE followed the potentials at which occurs, for both the electrolytes support that has been tested, D-(-)-tartaric acid 0.5 mM in KOH 0.1 mM aqueous solution and KOH 0.1 M aqueous solution. All the CVs are made with Ag/AgCl/KCl<sub>sat</sub> as RE and Pt as CE, with a scan rate of 50 mV/s

	NORTH POLE			
	D-(-)-tartaric acid 0.5 mM in KOH 0.1 M		KOH 0.1 M	
Test Name	J Anodic [A]	E Anodic [V]	J Anodic [A]	E Anodic [V]
CV01_Scan1	5.066E-04	0.600	3.719E-04	0.574
CV01_Scan3	4.323E-04	0.600	2.816E-04	0.562
CV01_Scan5	4.153E-04	0.600	2.825E-04	0.564
CV02_Scan1	7.373E-04	0.688	3.315E-04	0.669
CV02_Scan3	6.662E-04	0.674	4.292E-04	0.654
CV02_Scan5	6.560E-04	0.671	4.552E-04	0.654
CV03_Scan1	6.897E-04	0.674	5.014E-04	0.659
CV03_Scan3	6.323E-04	0.671	4.644E-04	0.657
CV03_Scan5	6.299E-04	0.671	4.687E-04	0.657
	SOUTH POLE			
	D-(-)-tartaric acid 0.5 mM in KOH 0.1 M		KOH 0.1 M	
Test Name	J Anodic [A]	E Anodic [V]	J Anodic [A]	E Anodic [V]
CV01_Scan1	3.83E-04	0.600	2.70E-04	0.600
CV01_Scan3	3.35E-04	0.600	1.79E-04	0.600
CV01_Scan5	3.20E-04	0.600	1.69E-04	0.600
CV02_Scan1	5.98E-04	0.674	3.32E-04	0.669
CV02_Scan3	5.41E-04	0.659	3.41E-04	0.645
CV02_Scan5	5.38E-04	0.659	3.41E-04	0.645
CV03_Scan1	6.06E-04	0.667	3.85E-04	0.649
CV03_Scan3	5.64E-04	0.664	3.80E-04	0.647
CV03_Scan5	5.77E-04	0.664	4.04E-04	0.649

Table III SI - Ratio of anodic current peaks in during CV of Ni electrodeposited on north and south pole of magnet B88X0 of K&J Magnetic, Inc used as WE with solution of 0.5 mM D-(-)-tartaric acid in KOH 0.1 M and KOH 0.1 M as electrolyte support. All the cyclic voltammetries are made with Ag/AgCl/KCl<sub>sat</sub> as RE and Pt as CE, with a scan rate of 50 mV/s. Last column shows the result of the sign function of the difference between the two values in the associated row (North – South)

	ANODIC CURRENT RATIO		sgn ( J <sub>ratio</sub> North - J <sub>ratio</sub> South)
	J <sub>ratio</sub> North	J <sub>ratio</sub> South	
Test Name	J <sub>Tart</sub> / J <sub>KOH</sub>	J <sub>Tart</sub> / J <sub>KOH</sub>	
CV01_Scan1	1.477	1.403	+
CV01_Scan3	1.561	1.672	–
CV01_Scan5	1.530	1.675	–
CV02_Scan1	1.507	1.736	–
CV02_Scan3	1.429	1.687	–
CV02_Scan5	1.358	1.591	–
CV03_Scan1	1.321	1.569	–
CV03_Scan3	1.331	1.532	–
CV03_Scan5	1.317	1.491	–
CV01_Scan1	1.362	1.415	–
CV01_Scan3	1.535	1.869	–
CV01_Scan5	1.470	1.890	–
CV02_Scan1	2.224	1.803	+
CV02_Scan3	1.552	1.586	–
CV02_Scan5	1.441	1.577	–
CV03_Scan1	1.376	1.573	–
CV03_Scan3	1.362	1.485	–
CV03_Scan5	1.344	1.426	–

*Table VIIISI – Table of the values of spin polarization (SP%) of the current in the measurement made with L-(+)-tartaric acid. The values used to calculate SP% are the ones recorded and reported in Table SI and Table SI for what concerns the current peaks. Table, instead, report the “anodic current ratio”.*

	ANODIC CURRENT RATIO		Spin Polarization Percentage in L-(+)-tartaric acid
	North Pole	South Pole	
Test Name	$J_{\text{Tart}} / J_{\text{KOH}}$	$J_{\text{Tart}} / J_{\text{KOH}}$	$\text{SP}\% = \frac{\left(\frac{J_{\text{Tart}}}{J_{\text{KOH}}}\right)_{\text{(North)}} - \left(\frac{J_{\text{Tart}}}{J_{\text{KOH}}}\right)_{\text{(South)}}}{\left(\frac{J_{\text{Tart}}}{J_{\text{KOH}}}\right)_{\text{(North)}} + \left(\frac{J_{\text{Tart}}}{J_{\text{KOH}}}\right)_{\text{(South)}}}$
CV01_Scan1	1.798	1.514	8.6%
CV01_Scan3	1.799	1.596	6.0%
CV01_Scan5	1.646	1.492	4.9%
CV02_Scan1	1.677	1.420	8.3%
CV02_Scan3	1.529	1.410	4.0%
CV02_Scan5	1.487	1.359	4.5%
CV03_Scan1	1.432	1.326	3.9%
CV03_Scan3	1.305	1.285	0.8%
CV03_Scan5	1.276	1.273	0.1%
CV01_Scan1	1.798	1.514	8.6%
CV01_Scan3	1.799	1.596	4.9%
CV01_Scan5	1.646	1.492	4.9%
CV02_Scan1	1.677	1.420	8.2%
CV02_Scan3	1.529	1.410	4.0%
CV02_Scan5	1.487	1.359	4.4%
CV03_Scan1	1.432	1.326	4.0%
CV03_Scan3	1.305	1.285	0.7%
CV03_Scan5	1.276	1.273	0.2%

*Table IXSI - Table of the values of spin polarization (SP%) of the current in the measurement made with D-(-)-tartaric acid. The values used to calculate SP% are the ones recorded and reported in Table IIISI and Table IVSI for what concerns the current peaks. Table VSI, instead, report the “anodic current ratio”.*

	ANODIC CURRENT RATIO		Spin Polarization Percentage in D-(-)-tartaric acid
	North Pole	South Pole	
Test Name	$J_{\text{Tart}} / J_{\text{KOH}}$	$J_{\text{Tart}} / J_{\text{KOH}}$	$\text{SP}\% = \frac{\left(\frac{J_{\text{Tart}}}{J_{\text{KOH}}}\right)_{\text{(South)}} - \left(\frac{J_{\text{Tart}}}{J_{\text{KOH}}}\right)_{\text{(North)}}}{\left(\frac{J_{\text{Tart}}}{J_{\text{KOH}}}\right)_{\text{(North)}} + \left(\frac{J_{\text{Tart}}}{J_{\text{KOH}}}\right)_{\text{(South)}}}$
CV01_Scan1	1.362	1.415	1.9%
CV01_Scan3	1.535	1.869	9.8%
CV01_Scan5	1.470	1.890	12.4%
CV02_Scan1	2.224	1.803	-10.4%
CV02_Scan3	1.552	1.586	1.1%
CV02_Scan5	1.441	1.577	4.5%
CV03_Scan1	1.376	1.573	6.7%
CV03_Scan3	1.362	1.485	4.3%
CV03_Scan5	1.344	1.426	2.9%
CV01_Scan1	1.477	1.403	-2.5%
CV01_Scan3	1.561	1.672	3.4%
CV01_Scan5	1.530	1.675	4.5%
CV02_Scan1	1.507	1.736	7.0%
CV02_Scan3	1.429	1.687	8.3%
CV02_Scan5	1.358	1.591	7.9%
CV03_Scan1	1.321	1.569	8.6%
CV03_Scan3	1.331	1.532	7.0%
CV03_Scan5	1.317	1.491	6.2%